H19 controls reactivation of the imprinted gene network during muscle regeneration

Clémence Martinet, Paul Monnier*, Yann Louault‡, Matthieu Benard, Anne Gabory§ and Luisa Dandolo¶

ABSTRACT

The *H19* locus controls fetal growth by regulating expression of several genes from the imprinted gene network (IGN). *H19* is fully repressed after birth, except in skeletal muscle. Using loss-of-function $H19^{\Delta 3}$ mice, we investigated the function of *H19* in adult muscle. Mutant muscles display hypertrophy and hyperplasia, with increased *Igf2* and decreased myostatin (*Mstn*) expression. Many imprinted genes are expressed in muscle stem cells or satellite cells. Unexpectedly, the number of satellite cells was reduced by 50% in $H19^{\Delta 3}$ muscle fibers. This reduction occurred after postnatal day 21, suggesting a link with their entry into quiescence. We investigated the biological function of these mutant satellite cells *in vivo* using a regeneration assay induced by multiple injections of cardiotoxin. Surprisingly, despite their reduced number, the self-renewal capacity of these cells is fully retained in the absence of *H19*. In addition, we observed a better regeneration potential of the mutant muscles, with enhanced expression of several IGN genes and genes from the IGF pathway.

INTRODUCTION

The *H19* gene produces an imprinted maternally expressed non-coding RNA (Brannan et al., 1990). This transcript is very abundant during murine embryonic development and is as highly expressed as β-actin (Poirier et al., 1991). A highly conserved stem-loop structure in the first exon of the gene was discovered to produce a microRNA, called miR-675 (Pfeifer and Tilghman, 1994; Smits et al., 2008). Distinct roles during embryogenesis were identified for the long non-coding RNA and for miR-675 (Gabory et al., 2009, 2010; Keniry et al., 2012). The production of mice carrying a targeted deletion of the gene, the $H19^{\Delta 3}$ strain, allowed us to identify an overgrowth phenotype in the absence of the *H19* gene. This phenotype is first detected in E15.5 embryos and continues in adult mice (Ripoche et al., 1997). Using both loss-of-function $H19^{\Delta 3}$ and gain-of-function *H19* transgenic ($H19^{Tg}$) animals, we identified nine other imprinted genes whose expression was increased in the absence of *H19* and was rescued by the transgene (Gabory et al., 2009). These genes belong to an imprinted gene network described by several authors (Varrault et al., 2006; Lui et al., 2008; Berg et al.,

2011; Al Adhami et al., 2015). Our results suggest that *H19* controls growth of the embryo through a balanced expression of imprinted genes.

We showed that this control of the imprinted gene network (IGN) in the embryo is driven by an interaction of the *H19* non-coding RNA with the MBD1 methyl-CpG binding protein. This complex directly affects the expression of *Igf2*, *Mest* (*Peg1*) and *Slc38a4*, by modulating the H3K9me3 histone marks on the differentially methylated regions (DMRs) of these genes (Monnier et al., 2013). This suggests that imprinted genes are subject to epigenetic mechanisms on their DMRs that convey a strict control of their expression to produce a fine-tuned regulation of embryonic growth.

miR-675 has been shown to negatively regulate placental growth at the late stages of gestation, by affecting the expression of *Igf1r*. Its excision from exon 1 and its processing by Drosha into a pre-miRNA is inhibited by the HuR protein in early gestation placenta as well as in the embryo (Keniry et al., 2012).

H19 is strongly repressed after birth in all murine tissues, but it remains expressed in skeletal muscle and heart in the adult, suggesting an important function in these tissues (Poirier et al., 1991). Interestingly, *H19* was also originally identified under the name of *MyoH* in the same selective screen that pinpointed *MyoD* as a key factor in muscular differentiation (Davis et al., 1987). Recently, it has also been observed that miR-675 promotes differentiation of myoblast cell lines (Dey et al., 2014).

Our aim was to investigate the role of *H19 in vivo* during adult myogenesis in our $H19^{\Delta 3}$ model. Myogenesis is determined by several myogenic regulatory transcription factors, the MRFs, which include Pax7, Pax3, Myf5, Myod, myogenin and Mrf4 (Sabourin and Rudnicki, 2000; Buckingham, 2007; Buckingham and Relaix, 2007). Muscles are composed of multinucleated myofibers, resulting from the differentiation of myoblasts under the control of these different MRFs. During embryogenesis, primary and secondary myogenesis result in the production of the myoblasts and myotubes composing the final adult muscle fibers. Satellite cells, characterized by the expression of *Pax7*, are located at the surface of the myofibers and were identified as muscle stem cells. The satellite cells appear and proliferate in the embryo at the end of gestation (E16.5) and their number is considered definitive around 21 days after birth. These satellite cells then enter into quiescence and remain in this state all through the adult life. However, they are activated upon injury of a muscle and contribute to the regeneration capacity of muscle tissue, by proliferation and differentiation steps in order to produce newly formed myofibers. This is accompanied by an important self-renewal step to help maintain this stem cell population (Sambasivan and Tajbakhsh, 2007; White et al., 2010). Interestingly, the IGN appears to play a role in the satellite cells as shown by the expression of many imprinted genes in these cells (Yan et al., 2003; Berg et al., 2011; Al Adhami et al., 2015).

Institut Cochin, INSERM U1016, CNRS UMR 8104, University Paris Descartes, Paris 75014, France.
*Present address: Institute of Molecular Health Sciences, Swiss Federal Institute of Technology, ETH, Zurich 8093, Switzerland. ‡Present address: Institut Curie, Unit 'Nuclear Dynamics' UMR 3664 CNRS, Paris 75248, Cedex 05, France. §Present address: UMR BDR, INRA, ENVA, University Paris Saclay, Jouy-en-Josas 78350, France.

¶Author for correspondence (luisa.dandolo@inserm.fr)

We show here that the overgrowth phenotype of the $H19^{\Delta 3}$ mice is associated with muscle hypertrophy and hyperplasia. This phenotype is linked with higher proliferation of $H19^{\Delta 3}$ myoblasts compared with wild-type (wt) myoblasts and with higher expression of $Igf2$ and reduced expression of myostatin ($Mstn$) in adult muscle. $H19$ is highly expressed in satellite cells and this led us to investigate the status of these cells in the mutant muscles. Unexpectedly, a 50% reduction in the number of satellite cells was observed in adult $H19^{\Delta 3}$ mice compared with wt controls. To evaluate the biological function of these satellite cells $in\ vivo$, we investigated their regeneration capacity and their self-renewal status.

RESULTS

$H19^{\Delta 3}$ muscles display hypertrophy and hyperplasia

$H19^{\Delta 3}$ mice display a general increase in mass of 8-10% compared with wt littermates (Ripoche et al., 1997; Gabory et al., 2009; Fig. S1). We linked this phenotype to muscle overgrowth because the tibialis anterior mass in $H19^{\Delta 3}$ mutants showed an increase of 25% compared with wt animals (6-week-old mice; Fig. 1A). To identify
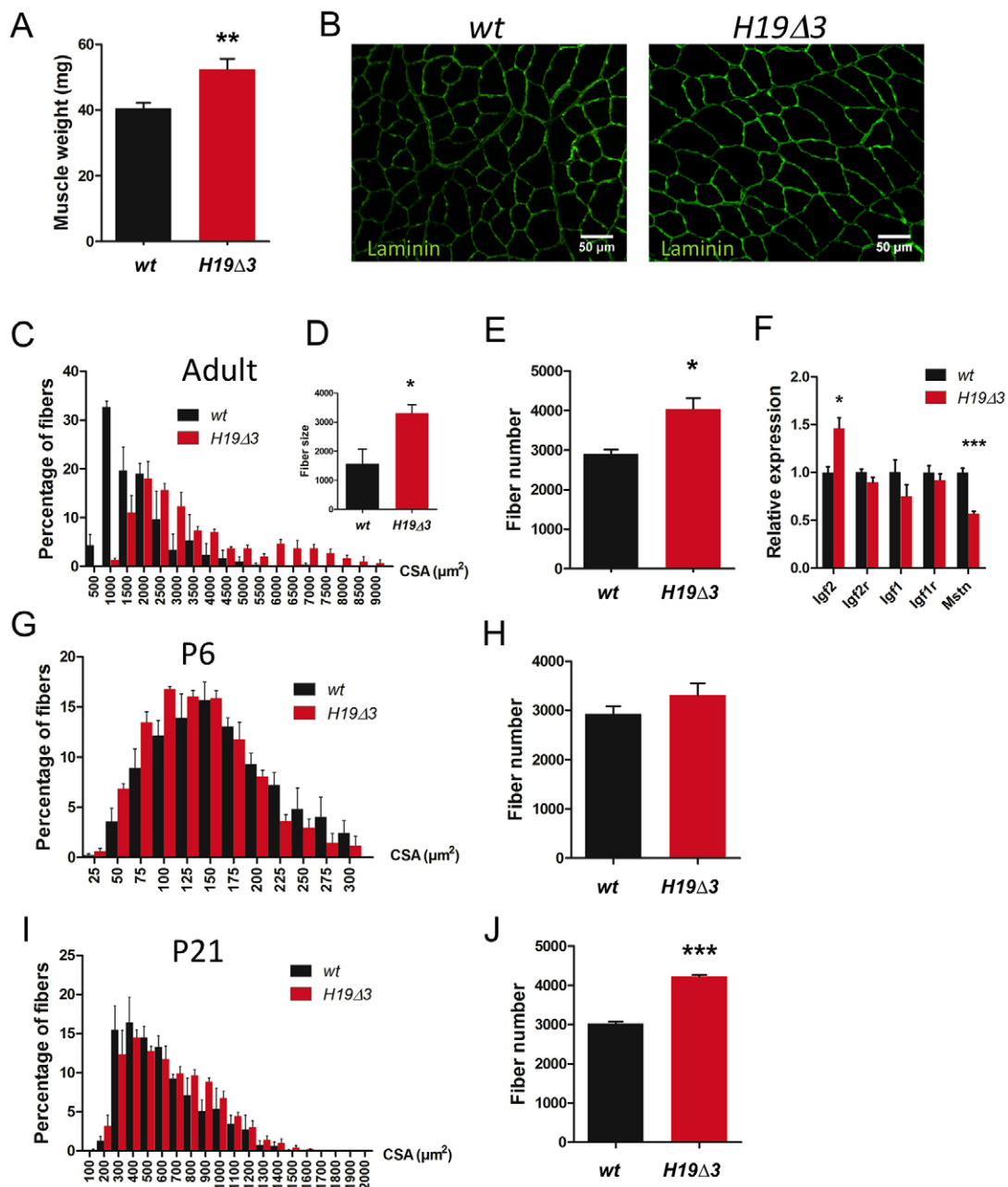

Fig. 1. $H19$ deletion induces muscle hyperplasia and hypertrophy. (A) Mass of individual tibialis muscles from wt and $H19^{\Delta 3}$ 6-week-old males (n=12 and n=15, respectively). (B) Histological section of tibialis muscle from wt and $H19^{\Delta 3}$ mice immunostained with anti-laminin antibody. (C) Histogram of fiber CSA (µm^2) from tibialis of adult males (n=3/genotype), mean of fiber CSA is also represented as a bar graph (D). (E) Number of fibers per tibialis section from adult males (n=3 mice/genotype). (F) Transcript levels of genes from the IGF pathway and of myostatin ($Mstn$) were quantified by RT-qPCR in adult tibialis muscle (n=4 mice/genotype). (G,I) Histograms of fiber CSA (µm^2) from tibialis of P6 males (n=4/genotype) (G), and of P21 males (n=3/genotype) (I). (H,J) Number of fibers per tibialis section from P6 males (n=4/genotype) (H), and from P21 males (n=3/genotype) (J). Data are shown as means±s.e.m. Asterisks indicate that data are statistically significant (*P<0.05, **P<0.01, ***P<0.001; Student's t-test). CSA, cross-section area.

the cause of this overweight phenotype, tibialis muscles were collected from 6-week-old male adults and sections were labeled with laminin (Fig. 1B). The cross-section area (CSA) was determined and showed both hypertrophy (2-fold increase, Fig. 1C,D) and hyperplasia (1.3-fold increase, Fig. 1E) of $H19^{\Delta 3}$ muscles compared with wt muscles.

To determine whether these phenotypes are established during the postnatal stage, tibialis muscles were collected from $H19^{\Delta 3}$ and wt mice at postnatal day (P) 6 and P21. No difference in the CSA between the mutant and the wt muscles was found at either of these stages; therefore, hypertrophy is only established after P21 (Fig. 1G, I). By contrast, hyperplasia begins earlier than hypertrophy: the number of fibers was slightly higher at P6, although the difference was not statistically significant (12% increase, P=0.24), but by P21, $H19^{\Delta 3}$ tibialis muscles showed significant hyperplasia (39% increase; Fig. 1H,J).

Two major signaling pathways control skeletal muscle growth: the insulin-like growth factor (IGF) pathway acts as a positive regulator of muscle growth, and the myostatin pathway acts as a negative regulator. To investigate these pathways, we performed expression analysis by RT-qPCR on wt and $H19^{\Delta 3}$ adult muscles. We identified an increase in the level of $Igf2$ expression (50% increase) and a reduction of $Mstn$ expression level (−50%) in the absence of $H19$ (Fig. 1F). Expression of other members of the IGF pathway such as $Igf2r$, $Igf1$ and $Igf1r$ showed no significant difference between $H19^{\Delta 3}$ and wt samples.

We concluded from these observations that hyperplasia is present at the postnatal stage. The number of muscle fibers is normally set between E18 and birth (White et al., 2010). Our results suggest that an increased proliferation leading to hyperplasia occurs in the $H19^{\Delta 3}$ muscles, probably during the late fetal stage. By contrast, hypertrophy sets in only at the adult stage in the mutant muscles. The expression profiles of $Igf2$ and $Mstn$ strongly suggest that these genes are responsible for the hypertrophic phenotype of the mutant mice.

H19 deletion induces depletion of satellite cells

Because many imprinted genes, including *H19*, are expressed in satellite cells, we investigated whether the absence of *H19* would have an effect on these cells. We first evaluated the expression of *Pax7* – a specific marker of satellite cells – in whole tibialis muscles by RT-qPCR (Fig. 2A). Interestingly, there was a significant decrease (−35%) in the expression of this gene in $H19^{\Delta 3}$ muscles compared with wt muscles.

We then compared the number of satellite cells present on muscle fibers from $H19^{\Delta 3}$ and wt mice. For these experiments, the extensor digitorum longus (EDL) muscle was used because of easier dissection of the muscle held by the tendon. Individual fibers were immunostained with anti-Pax7 antibodies and DAPI counterstaining (Fig. 2B). The number of satellite cells present on fibers showed a striking 50% reduction in adult $H19^{\Delta 3}$ fibers, compared with wt fibers (Fig. 2C). In addition to this experiment, the number of satellite cells was compared in muscle fibers from $H19^{−/+}$, wt and $H19^{−/+};Tg$ littermates. The results showed a similar, although less pronounced, decrease in the number of satellite cells (−25%) in $H19^{−/+}$ compared with wt muscle (Fig. 2D). The difference in the number of satellite cells in the two experiments is probably due to the different backgrounds on which these mice were maintained, 129/SV for the first and C57BL/6/CBA/129 for the experiment including the transgene. Interestingly, in $H19^{−/+};Tg$ mice, the presence of the *H19* transgene was able to rescue the reduced number of satellite cells and restored values similar to counts in wt muscles.

Because satellite cells develop during late gestation and continue to proliferate during the postnatal stage up to P21, we performed anti-Pax7 labeling on P6 and P21 muscles. For the P21 stage, individual fibers were isolated from the EDL muscle and immunostained with anti-Pax7 antibodies and DAPI as above (Fig. 2E). For the P6 stage, because of the small size of the muscle samples, Pax7 detection was performed on frozen sections and included a co-labeling with anti-laminin antibodies and DAPI counterstaining (Fig. 2F,G). A comparison of $H19^{\Delta 3}$ and wt muscles showed no difference in the number of satellite cells at these early stages. The reduction in the number of satellite cells therefore occurs during adult life. This could suggest that the establishment of quiescence is delayed in the mutant mice, with $H19^{\Delta 3}$ satellite cells continuing to be incorporated and fused into muscle fibers later than the P21 stage and thus reducing their number in the adult muscle.

To investigate this, we performed simultaneous Ki67 and Pax7 immunostaining at the P21 stage, when the satellite cells enter into quiescence (Fig. 2H,I). The ratio of Pax7$^+$/Ki67$^+$ versus Pax7$^+$/Ki67$^-$ at this stage shows the ratio of active satellite cells to quiescent cells. The number of active satellite cells was higher in the $H19^{\Delta 3}$ P21 sections. This suggests that the $H19^{\Delta 3}$ satellite cells have not yet reached full quiescence at this stage, reinforcing the idea that entry into quiescence is delayed in the mutants compared with wt muscles.

H19 controls proliferation of myoblasts

Since the fate of satellite cells is to proliferate, differentiate and self-renew, we first evaluated the proliferation capacity of $H19^{\Delta 3}$ myoblasts compared with wt myoblasts. Primary myoblasts were isolated from limb muscles of $H19^{\Delta 3}$ and wt adult mice. The myoblasts were maintained in culture in growth medium. Their growth rate was evaluated for 7 days and by day 7, the cell number had doubled in cells lacking *H19* compared with wt myoblasts (Fig. 3A). We then used the gain-of-function transgenic mice and isolated myoblasts from wt, $H19^{−/+}$ and $H19^{−/+};Tg$ littermates. We observed a rescue of the enhanced growth rate of the $H19^{−/+}$ myoblasts in the presence of the *H19* transgene (Fig. 3B). This suggests that the *H19* RNA itself is controlling myoblast number.

$H19^{\Delta 3}$ satellite cells show normal regeneration capacity

To evaluate the biological function of the satellite cells *in vivo*, we investigated their capacity to perform muscle regeneration. Quiescent satellite cells are activated after muscle injury and participate in the production of new myofibers. Injection of snake venom (cardiotoxin, Ctx) into the tibialis muscle induces injury of the muscle and allows to evaluate the regeneration capacity of satellite cells *in vivo*. We performed a first Ctx injection in tibialis muscles from $H19^{\Delta 3}$ and wt male mice and collected injured muscles 4 weeks later. Sections of the injured muscles were stained with Hematoxylin and Eosin. The sections displayed normal muscle fibers with centrally located nuclei and there were no differences in regeneration capacity at this stage between $H19^{\Delta 3}$ and wt samples (Fig. 4B, Fig. S2).

Repeated injury is a suitable model to assess the self-renewal ability of satellite cells and the long-term regeneration potential of skeletal muscle. We reasoned that if $H19^{\Delta 3}$ satellite cells had a self-renewal defect, multiple injections of Ctx would lead to poor regeneration after several rounds of injury. To investigate this question, we performed four series of injections of Ctx into the tibialis muscle of 6-week-old adult male mice, each separated by a period of 28 days (Fig. 4A). The experiment was repeated three
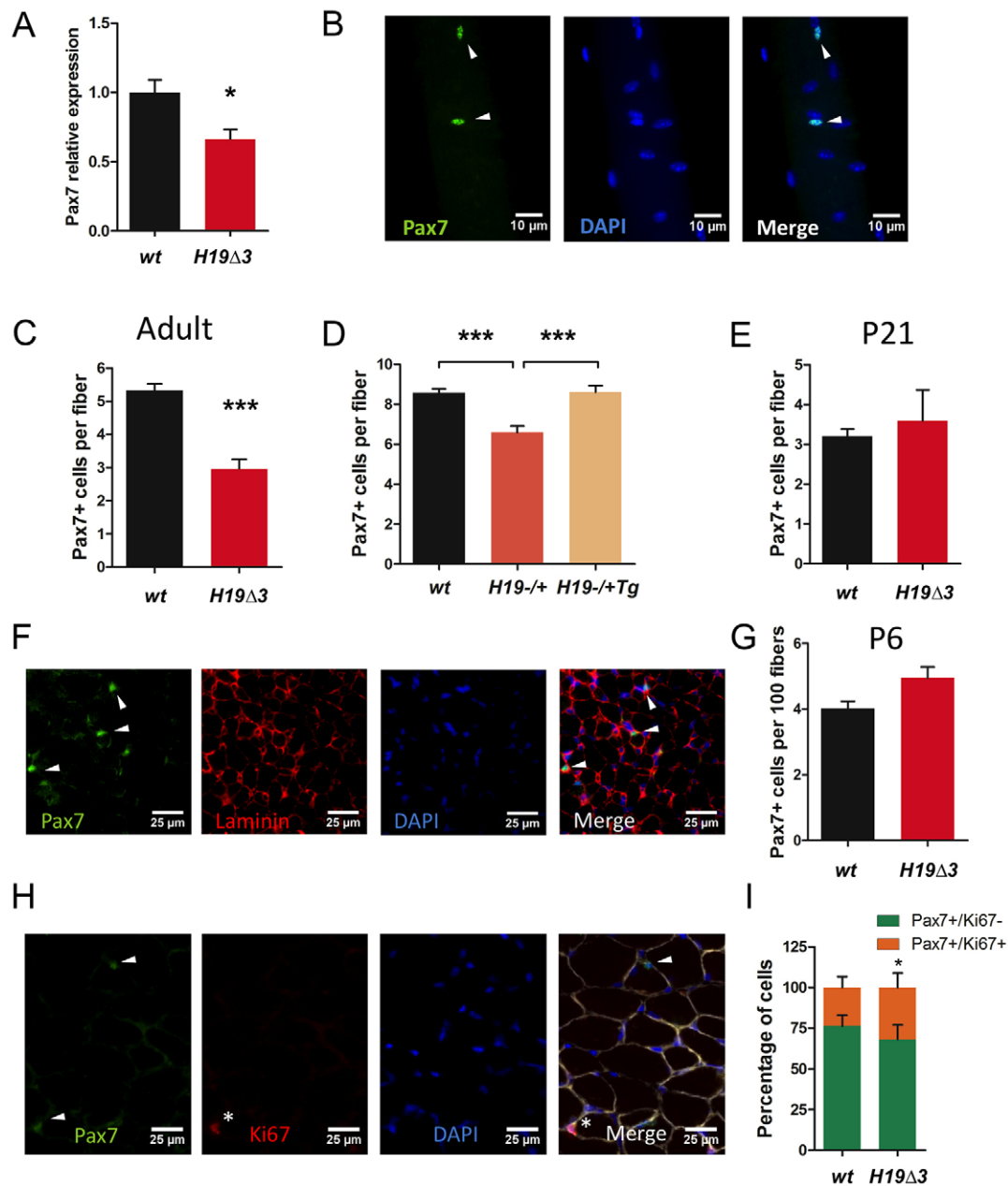
Fig. 2. *H19* controls the number of satellite cells. (A) Transcript level of the *Pax7* gene was quantified by RT-qPCR in adult tibialis muscle (*n*=4 mice/genotype). (B) Immunostaining of satellite cells. Arrowheads indicate Pax7^{+} cells (green) on isolated myofibers. Nuclei are counterstained with DAPI (blue). (C) Mean number of satellite cells per EDL myofiber of wt and *H19*[Δ3] adult mice (*n*=mean of 130 fibers from four mice/genotype). (D) Mean number of satellite cells per EDL myofiber of wt, *H19*^{−/+} and *H19*^{−/+};*Tg* adult mice (*n*=4 mice/genotype). (E) Mean number of satellite cells per EDL myofiber of wt and *H19*[Δ3] P21 mice (*n*=3 mice/genotype). (F) EDL cryosection from P6 males immunostained with Pax7 (green) and laminin (red) antibodies. Nuclei are counterstained with DAPI (blue). Arrowheads indicate Pax7^{+} cells. (G) The mean number of Pax7^{+} cells per 100 fibers/section represented as a bar graph (*n*=4/genotype). (H) *EDL* cryosection from P21 males immunostained with Pax7 (green) and Ki67 (red) antibodies. Nuclei are counterstained with DAPI. Laminin staining is shown in white in the merged image. Arrowheads indicate only Pax7^{+} cells. Stars indicate Pax7^{+}/Ki67^{+} positive cells. (I) The ratio of Pax7^{+}/Ki67^{+} versus Pax7^{+}/Ki67^{−} cells from either wt or *H19*[Δ3] sections is represented as a bar graph (*n*=4/genotype). Data are shown as means±s.e.m. Asterisks indicate that data are statistically significant [*$P<0.05$, ***$P<0.001$; Student's *t*-test (A,C,E,G,I) and Kruskal–Wallis test with Dunn's post test (D)].

times on 5-6 mice of each genotype in each experiment. After the third injection, muscles were collected after 28 days and sections were stained with Hematoxylin and Eosin. Regeneration was complete and very similar to what was observed after only one injection, suggesting that self-renewal of the satellite cells occurred normally in the mutant muscles.

It was described previously that the strongest change in gene expression is detected 7 days after injury (Andersen et al., 2013; Al

Adhami et al., 2015). Therefore, muscles were also collected at 7 days after the fourth injection. Interestingly, the injured *H19*[Δ3] muscles were larger than the wt injured muscles (Fig. 4C). A 12% increase in mass was observed for the mutant injured muscle compared with the wt injured muscle (Fig. 4D; *n*=11, *P*=0.0128).

Sections of these injured muscles showed similar regeneration efficiency, with centrally located nuclei. We performed anti-laminin immunolabeling on these muscle sections and evaluated the number
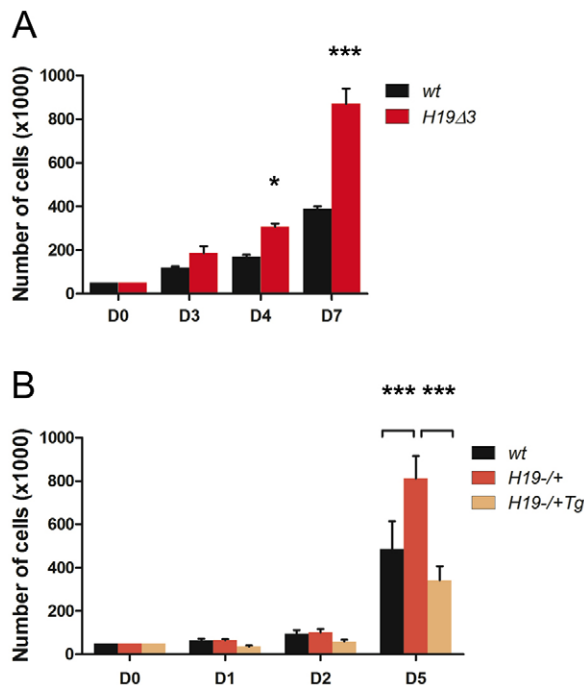
Fig. 3. *H19* controls myoblast growth. Growth curves for (A) wt and *H19*$^{\Delta 3}$ primary myoblast cultures (from two mice per genotype and triplicate time points) and (B) wt, *H19*$^{-/+}$ and *H19*$^{-/+}$;*Tg* primary myoblast cultures (from three mice per genotype and triplicate time points). Data are shown as means±s.d. Asterisks indicate that data are statistically significant (*$P<0.05$, ***$P<0.001$; two-way ANOVA, Bonferroni post test).

of fibers and their CSA. No difference in the ratio of Ctx/control number of fibers between wt and *H19*$^{\Delta 3}$ muscles was detected. By contrast, a small percentage of fibers were larger in *H19*$^{\Delta 3}$ compared with the wt muscles (Fig. 4E).

Expression levels of *Pax7* and *Ki67* (also known as *Mki67*) were analyzed by RT-qPCR on samples collected 7 days after the fourth injection (Fig. 4F). Higher expression levels of these two genes (1.5-fold and 2-fold increase, respectively) were detected in the mutant samples compared with the wt samples. This suggests that although there are fewer satellite cells in the mutant muscle, *H19*$^{\Delta 3}$ satellite cells are correctly activated after injury and even show increased proliferation compared with wt cells during the regeneration process. This is in agreement with the increased growth rate of mutant myoblasts compared with wt myoblasts, observed *in vitro* in the primary cultures (Fig. 3).

To investigate the reason for the increased mass and size of *H19*$^{\Delta 3}$ regenerated muscles, expression levels of genes involved in growth control were analyzed. Whereas in uninjured muscle, only *Igf2* expression was increased in mutants, others genes of the IGF pathway – *Igf1*, *Igf1r* and *Igf2r* – showed higher expression levels (1.5-fold increase) in the mutant samples after injury (Fig. 4G). This upregulation of IGF pathway genes certainly accounts for the increased muscle mass and the hypertrophic fibers observed after the multiple Ctx injuries.

We concluded from these results that the *H19*$^{\Delta 3}$ satellite cells have a self-renewal capacity that is similar to that of wt satellite cells. Regeneration occurs normally in mutant mice, if not better than in wt mice. The mass increase observed for the regenerated mutant muscles could be associated with the increased proliferation of the *H19*$^{\Delta 3}$ myoblasts (suggested by the increase in *Ki67* expression) and with hypertrophic fibers with high levels of expression of genes from the growth-controlling IGF pathway.

Imprinted gene network expression is induced upon muscle regeneration

Imprinted genes are co-expressed and co-regulated in fetal tissues and belong to an IGN. We had shown previously that *H19* controlled nine genes of the IGN during fetal development (Gabory et al., 2009; Monnier et al., 2013). To identify potential genes involved in the *H19* mutant muscle phenotype described above, we performed RT-qPCR experiments on muscles collected at different stages from *H19*$^{\Delta 3}$ and wt mice. Several genes from the IGN were tested, such as *Igf2*, *Dlk1*, *Cdkn1c*, *Dcn*, *Peg3*, *Mest*, *Igf2r* and *Slc38a4*.

No major significant alteration of expression was observed in muscles collected from P6 mice, with the exception of *Igf2* and *Dlk1* (15-20% increase; Fig. 5A). We also tested P21 proliferating myoblast cultures and found no change in expression of any of these genes (Fig. S3). This suggests that the effect of the *H19* gene on the modulation of the IGN occurs essentially in the embryo as we had shown previously (Gabory et al., 2009) and not at postnatal stages. In adult muscles, *Igf2* expression remained upregulated (+50%) and was accompanied by a decrease in expression of *Dcn* and *Slc38a4* (−20% and −50%, respectively; Fig. 5B). The reduction in *Dcn* expression can be correlated with the observed decrease in *Mstn* expression levels (Fig. 1F), because both genes are involved in the TGF-β pathway (Kishioka et al., 2008).

We then performed the same analysis of these imprinted genes on uninjured and injured tibialis muscles, collected at 7 days after four rounds of Ctx injury. We first evaluated a possible effect of Ctx treatment on the reference genes and found no significant difference in their expression between control and Ctx samples (Fig. S4). A comparison of the expression profiles of the imprinted genes in wt mice showed a striking increase in levels of expression of *H19* (6-fold), *Igf2* (46-fold), *Dlk1* (4.5-fold), *Cdkn1c* (2-fold), *Peg3* (8-fold), *Mest/Peg1* (10-fold) and *Igf2r* (1.5-fold) (Fig. 5C, Fig. S5). In the *H19*$^{\Delta 3}$ injured muscles, a further enhancement of expression was detected for *Dlk1* (3.4-fold), *Cdkn1c* (2-fold), *Dcn* (1.5-fold), *Peg3* (2-fold) and *Igf2r* (1.6-fold; Fig. 5D and Fig. S5). For the evaluation of *Dlk1* expression, primers for both the membrane-bound and soluble forms of Dlk1 were used and produced very similar results. We concluded from these results that *H19* and a set of genes from the IGN are strongly reactivated during regeneration and formation of new myofibers in adult muscle.

DISCUSSION

H19 plays an important role during development in limiting growth of the embryo via a regulatory control of genes belonging to the IGN (Gabory et al., 2009, 2010). Since *H19* remains expressed in the adult muscle, the *H19*$^{\Delta 3}$ mutant mice provide an interesting model to study the role of this gene in the adult. Our main findings show a role for the *H19* gene in the control of the number of satellite cells and of their proliferation in the adult muscle. We also show an effect of the *H19* gene in the process of muscle regeneration, in a functional test of multiple rounds of injury. Interestingly, the analysis of the expression of imprinted genes from the IGN revealed a remarkable upregulation of these genes during regeneration accompanied by increased muscle size in the mutant mice. Our study of the *H19*$^{\Delta 3}$ mice provides a model for the regulation of the IGN in the context of muscle injury. This suggests that the embryonic regulatory function of *H19* on the IGN is reactivated during the regeneration process occurring in the adult muscle.

Our first observation was an increase in the mass of the *H19*$^{\Delta 3}$ muscles with hypertrophy and hyperplasia at the adult stage, compared with wt mice. Muscle fiber number is determined during
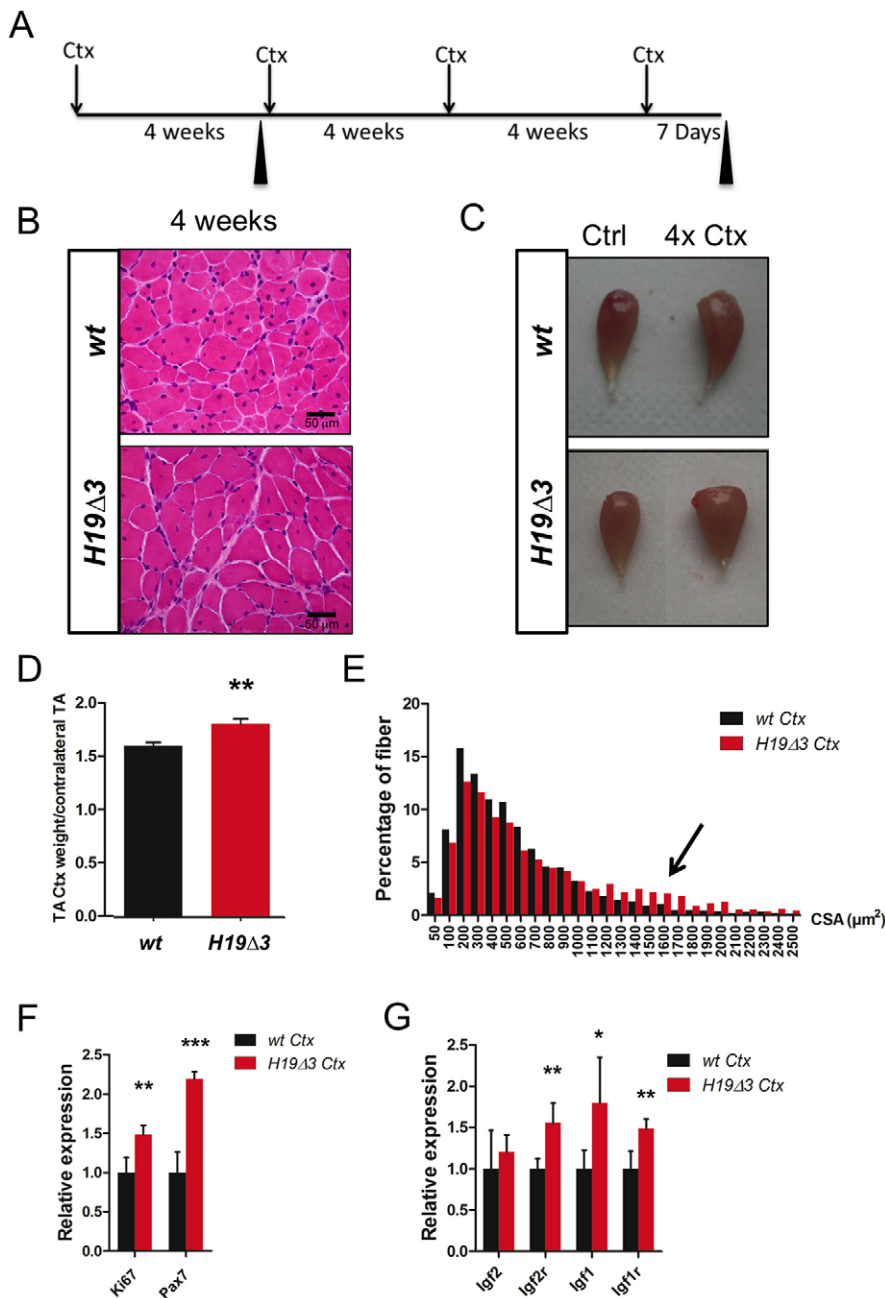
Fig. 4. Regeneration assay by cardiotoxin (Ctx) injection. (A) Representation of the multiple Ctx injection assay. Arrowheads indicate time of collection of the muscles. (B) Sections of adult tibialis muscle from wt and $H19^{\Delta3}$ mice after one Ctx injection stained with Hematoxylin and Eosin. (C) wt and $H19^{\Delta3}$ muscles after four Ctx injections, with control contralateral uninjected muscle. (D) Mass of injured tibialis versus contralateral uninjected tibialis from wt and $H19^{\Delta3}$ males (n=11). (E) Histogram of fiber CSA (μm²) after four Ctx injections in wt and $H19^{\Delta3}$ muscles. Arrow points to larger fibers in the mutant muscle. Transcript levels of (F) *Pax7* and *Ki67* genes and (G) the IGF pathway genes quantified by RT-qPCR in adult wt and $H19^{\Delta3}$ injured tibialis muscles (n=4 mice/genotype). Data are shown as means±s.e.m. Asterisks indicate that data are statistically significant (*$P<0.05$, **$P<0.01$, ***$P<0.001$; Student's *t*-test).

development at the secondary myogenesis step, which occurs during late gestation and the total number of fibers is unchanged between birth and adult stage (White et al., 2010). We suggest that the increased proliferation observed in $H19^{\Delta3}$ myoblasts compared with wt myoblasts must occur during the late fetal stage. This leads to the hyperplasia observed in adult muscle. Muscle fiber size, by contrast, is under the control of growth-controlling genes (Musarò et al., 2001). Hypertrophy observed in the adult mutant muscles could therefore be correlated to the increase in the expression levels of *Igf2* and *Dlk1*, combined with the reduced expression of *Mstn*. Our initial experiments in the $H19^{\Delta3}$ embryos had revealed an upregulation of *Igf2* in the absence of *H19* (Ripoche et al., 1997). *Igf2* belongs to the IGF pathway, which confers positive growth regulation. Interestingly, *Igf2* expression is normally downregulated after birth and is replaced by expression of *Igf1*. In the case of the $H19^{\Delta3}$ mutants, the absence of *H19* seems to help maintain *Igf2*

expression in adult muscle. *Dlk1* is another imprinted gene whose expression is enhanced in $H19^{\Delta3}$ muscle, at least at the P6 stage. *Dlk1* is highly induced during normal muscle development and during regeneration (Andersen et al., 2009; Waddell et al., 2010). *Dlk1* is also one of the genes responsible for the callipyge phenotype in cattle (Charlier et al., 2001) and has been shown to induce hypertrophy (Davis et al., 2004; Waddell et al., 2010). One of the other main regulatory pathways of muscle growth is the myostatin pathway. *Mstn*-null mice show hypertrophy and hyperplasia of their muscles (Lee and McPherron, 2001). Exceptional muscle development of the Belgian Blue cattle has also been associated with a mutation in *Mstn* (Grobet et al., 1997). Myostatin is considered to be a powerful inhibitor of muscle growth. Its reduced expression in the $H19^{\Delta3}$ muscles suggests that it could be a good candidate for the overgrowth phenotype of these mutants. A tight correlation between *Mstn* and *Igf2* expression has been
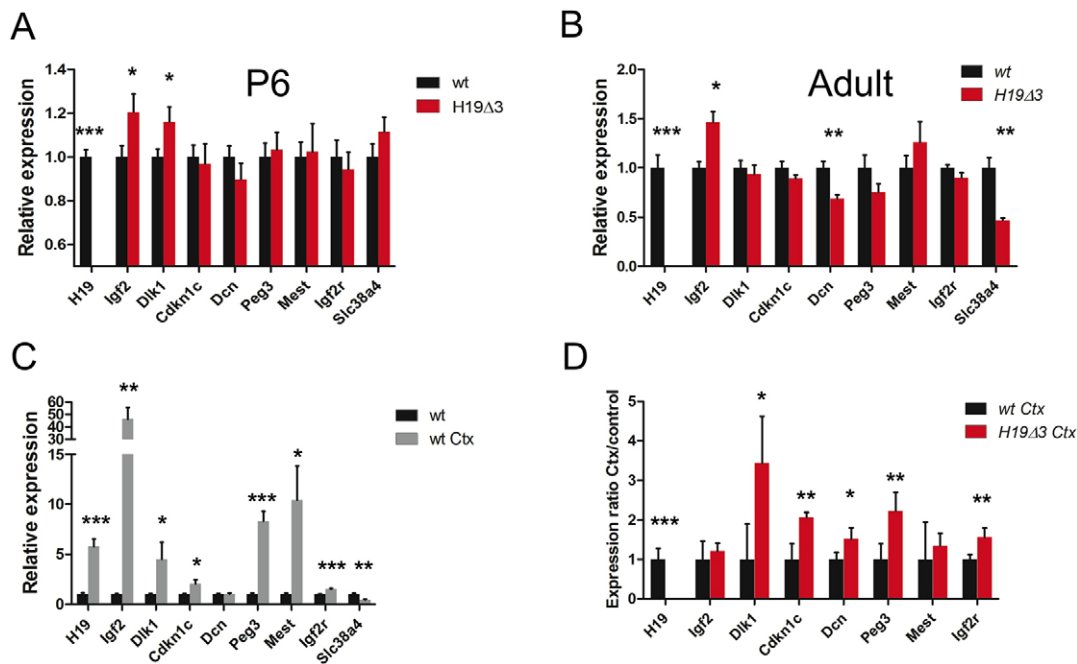
Fig. 5. IGN expression is induced upon muscle regeneration. (A) Transcript levels of the IGN genes in wt and $H19^{\Delta3}$ tibialis muscles from P6 mice, (B) in uninjured wt and $H19^{\Delta3}$ adult tibialis muscles, (C) in uninjured wt compared with injured wt Ctx adult tibialis muscles and (D) in injured wt Ctx compared with injured $H19^{\Delta3}$ Ctx reported to uninjured muscle transcript levels. Data are shown as means±s.e.m. Asterisks indicate that data are statistically significant (*$P<0.05$, **$P<0.01$, ***$P<0.001$; Student's t-test).

previously established (Kalista et al., 2012; Clark et al., 2015). Taken together, although other genes might also participate in this phenotype, we suggest that the upregulation of the growth-promoting *Igf2* and *Dlk1* genes at the early postnatal P6 stage coupled with the reduced expression of *Mstn* in the adult muscle are good candidates for the hypertrophic phenotype observed in the $H19^{\Delta3}$ mutant muscles.

Primary myoblasts in culture show an enhanced growth rate in the absence of *H19*, which can be rescued by the *H19* transgene. Although we have not pursued this study to identify the possible underlying mechanisms, this can be correlated with our previous identification of *H19* acting as a tumor suppressor (Yoshimizu et al., 2008). We surprisingly observed a 50% reduction in the number of satellite cells present on the mutant muscle fibers. Satellite cells are produced during late gestation and proliferate during the early postnatal period. They cease proliferating and enter into quiescence around 21 days after birth, with their number remaining constant after this stage (Schultz et al., 1978; White et al., 2010). To understand the reason for this reduction, we compared the number of satellite cells in wt and mutant muscle fibers at different postnatal stages, P6 and P21, and found no difference. The reduction in the number of satellite cells was only observed in the adult muscle. The rescue of the number of satellite cells in the $H19^{-/+};Tg$ strongly suggests that the *H19* gene is involved in the control of the number of satellite cells at some stage of their establishment.

H19 has previously been shown to affect quiescence of another category of stem cells – the hematopoietic stem cells (Venkatraman et al., 2013). A possible explanation for the observed reduction is that the entry into quiescence of satellite cells is delayed in $H19^{\Delta3}$ mutants. The number of satellite cells is normally fixed at a certain stage, but the mutant cells might continue to be incorporated into adult muscles after P21 and only enter into quiescence at a later stage. This would lead to a reduced number of quiescent satellite cells in the adult mutant muscle. Our experiment showing a higher

level of $Pax7^+/Ki67^+$ satellite cells in the mutant P21 muscles confirms this delay in the entry into quiescence. Quiescence perturbation could be a common feature of stem cells deficient for the *H19* gene.

At the molecular level, satellite cells might show a delay in their entry into quiescence because a certain number of genes involved in proliferation are not properly downregulated in the satellite cells. A comparison of expression profiles of quiescent and activated satellite cells reveals a strong induction of several imprinted genes upon activation (Pallafacchina et al., 2010). These genes are *Mest*, *Ndn*, *Cdkn1c*, *Gnas*, *Kvlqtot1* (all approximately 3- to 4-fold induction), *Slc38a4*, *Peg12*, *Igf2* (6-fold induction) and especially *Dlk1* (30- to 50-fold induction). If genes such as *Igf2* and *Dlk1* are not correctly repressed in the active $H19^{\Delta3}$ satellite cells at the time of their entry into quiescence, this could lead to continued proliferation and would result in a delay in the time to quiescence in the mutant muscles.

Satellite cells display stem cell properties of self-renewal, proliferation and differentiation. To further investigate the biological capacities of *H19*-deficient satellite cells, we focused on the regeneration capacity of these cells by injuring tibialis muscles. A first injection of Ctx resulted in efficient regeneration after 28 days both in wt and $H19^{\Delta3}$ injured muscles. A delay in the regeneration efficiency at early times (14 days post injury) has been observed (Dey et al., 2014). We also observed this delay in the $H19^{\Delta3}$ injured muscles as early as day 7, but regeneration appeared to be rescued with time. This delay could be an initial reflection of the reduced number of satellite cells. As muscle repair proceeds, more efficient proliferation of the $H19^{\Delta3}$ myoblasts compensates the reduced number of satellite cells and results in efficient regeneration after 28 days. Subsequent multiple rounds of injury show that the mutant satellite cells continue to perform their function and maintain a high capacity for muscle repair. A significant increase in the mass of *tibialis* muscles after four rounds of Ctx injury was

observed in $H19^{\Delta3}$ mice. This improvement could be related not only to the higher growth rate of mutant myoblasts but also to the enhanced expression of genes from the IGF pathway, because $Igf1$ has been shown to play a role in improving regeneration (Pelosi et al., 2007). Overall, the self-renewal capacity of the $H19$-deficient satellite cells does not seem to be impaired, and once activated, their efficient proliferation capacity leads to improved regeneration.

We followed the expression levels of genes from the IGN in whole muscle at the P6 and adult stage, in P21 myoblast cultures and during regeneration experiments. Very few genes were affected during postnatal growth and at the adult stage in $H19^{\Delta3}$ whole muscle. By contrast, in wt Ctx-injured muscles, seven imprinted genes showed increased expression ($H19$, $Igf2$, $Dlk1$, $Cdkn1c$, $Peg3$, $Mest$ and $Igf2r$). The involvement of genes from the IGN in regeneration has been previously described (Yan et al., 2003; Al Adhami et al., 2015). Our data provide a detailed quantification of the increased expression of IGN genes during wt regeneration. The strong increase in expression of $H19$ and $Igf2$ after injury can be related to the observed twofold increase in the expression of $Myod$ (Fig. S6). This myogenic factor binds the mesodermal enhancers controlling expression of the $H19$-$Igf2$ locus (Cao et al., 2010; Borensztein et al., 2013). Therefore, an increase in $Myod$ expression is expected to lead to a correlated increase in the expression of these two imprinted genes. In addition, we observe an enhanced upregulation of most imprinted genes in the mutant injured mice compared with the wt injured mice. In the embryo, the absence of $H19$ also induces upregulation of these genes, suggesting that the IGN is subject to a fine-tuned control to achieve correct development of the embryo (Gabory et al., 2009). The regenerating muscle is recapitulating an embryonic program, as evidenced by the expression of embryonic forms of myosin heavy and light chains in new myofibers (Whalen et al., 1990; Jerkovic et al., 1997). There is strong evidence for maternally expressed genes to limit growth, whereas paternally expressed genes enhance growth (Haig, 2004). A coordinated upregulation of these genes during regeneration therefore provides a simultaneous balanced correlation between growth enhancement and growth reduction. This results in adequately controlled muscle production. Enhanced expression of these genes during regeneration in $H19^{\Delta3}$ muscles could explain the improved regeneration effect in the mutant mice after multiple rounds of injury, although an important role for the IGF pathway must also be taken into account.

The $H19$ locus produces a long non-coding full-length RNA and a microRNA, miR-675. In placenta, miR-675 is shown to control growth by repressing $Igf1r$, a direct target of the miR (Keniry et al., 2012). It was also previously shown that the miR-675 plays a role in inducing differentiation of myoblasts (Dey et al., 2014). During enhanced regeneration of $H19^{\Delta3}$ muscles, $Igf1r$ expression is clearly upregulated, suggesting that the miR-675 might be responsible for part of this effect. Interestingly, a study performed on purified satellite cells has shown that miR-675 is not expressed in quiescent satellite cells but is expressed in activated satellite cells (D. Castel and S. Tajbakhsh, personal communication). Alternatively, since the $H19$ RNA interacts with MBD1 to bring H3K9me3 repressive marks on some of its targets ($Igf2$, $Mest$ and $Slc34a8$), $H19$ could act by repressing imprinted genes involved in the myogenic pathways through epigenetic modifications (Monnier et al., 2013). Another long non-coding RNA, $linc$-$MD1$, plays an important role in myogenesis, by targeting a myomiR called miR-133 (Legnini et al., 2014). Because the $H19$ RNA has also been shown to act as a sponge for $let7$ (Kallen et al., 2013), it could also interfere with the levels of other myomiRs. Whether the different effects of the $H19$

locus on the control of the number and growth rate of satellite cells and on regeneration efficiency can be attributed to the full-length RNA or to miR-675 remains to be elucidated.

Finally, the $H19$-$Igf2$ locus is associated in humans with the Beckwith-Wiedemann syndrome, in which affected children show an increased predisposition to tumors such as Wilms' tumors and rhabdomyosarcomas. This occurs particularly in cases of paternal unidisomies, and therefore is correlated with a lack of maternally expressed genes (such as $H19$) of the region (Cooper et al., 2005). $H19$ has been shown to be a tumor suppressor (Hao et al., 1993; Yoshimizu et al., 2008). The enhanced muscle regeneration observed in our mutant mouse model could be considered as a first step of increased proliferation of myofibers lacking $H19$, possibly leading to tumorigenesis. However, we have never observed tumors in our $H19^{\Delta3}$ mouse colony over the years. Provided the mouse model can be applied to a human situation, this suggests that occurrence of rhabdomyosarcomas requires the absence of more than one tumor suppressor gene in children with Beckwith-Wiedemann syndrome.

MATERIALS AND METHODS

Mouse strains
All experimental designs and procedures were in agreement with the guidelines of the animal ethics committee of the Ministère de l'Agriculture (France). $H19^{\Delta3}$ and $H19^{Tg}$ gain-of-function mice were previously described (Ripoche et al., 1997; Gabory et al., 2009). The $H19^{\Delta3}$ strain is maintained on the 129SV/Pas background. Mutant $H19^{\Delta3}$ females were mated with $H19^{Tg}$ males (C57BL/6/CBA background) to obtain $H19^{-/+};Tg$ mice. $H19^{-/+};Tg$ females were mated with wt males to obtain litters of $H19^{-/+}$, $H19^{-/+};Tg$ and wt mice on a similar genetic background. $H19^{-/+}$($H19^{mat\ \Delta3/pat\ wt}$) mice are identical to $H19^{-/-}$ mice because of the imprinted status of the gene.

Histology and immunostaining
Tibialis anterior and EDL muscles of P6, P21 or 6-week-old male mice from each genotype were dissected and fixed for 4 h at 4°C in 4% paraformaldehyde (PFA) and washed in PBS as described previously (Le Grand et al., 2012). After incubation in PBS and 10% sucrose overnight at 4°C, samples were incubated in PBS with 10% gelatin and 10% sucrose, then 10% gelatin and frozen in isopentane cooled by liquid nitrogen. Sections were obtained (7 μm) using a Leica CM1850 cryostat and stained with Hematoxylin and Eosin or immunostained using anti-Pax7 (Santa Cruz, sc-81648; 1:100), anti-Ki67 (Abcam, ab15580; 1:400) and anti-laminin (Santa Cruz, sc59854; 1:100) antibodies. Secondary antibodies were Alexa Fluor 488 anti-mouse IgG, Alexa Fluor 546 anti-rabbit IgG and Alexa Fluor 647 anti-rat IgG (Life Technologies). The sections were mounted and the images were captured with an Olympus BX63 microscope. Image analysis was performed with ImageJ (NIH) software.

Single myofiber isolation and staining
Single myofibers were isolated from the EDL muscles of P21 or 6-week-old male mice as previously described (Pasut et al., 2013). Freshly isolated fibers were fixed in 4% PFA, blocked in PBS containing 5% horse serum and 0.5% Triton X-100 for 1 h at room temperature and stained with anti-Pax7 antibodies (Santa Cruz, sc-81648; 1:100) at 4°C overnight. The samples were washed in PBS and incubated with secondary antibody Alexa Fluor 488 anti-mouse IgG (Life Technologies). Nuclei were counterstained with DAPI.

Primary myoblast isolation and cell proliferation assay
Primary myoblasts were isolated from limb muscles of P21 and 6-week-old male mice as described previously (Le Grand et al., 2012). For the adult 129SV/Pas wt and $H19^{\Delta3}$ cultures, two mice for each genotype were dissected. For the P21 mice, four mice for each genotype were dissected. For the C57BL/6/CBA background, three mice for each genotype were used.

Muscles were digested in collagenase B (10 mg/ml)/dispase (3.2 mg/ml) (Roche) at 37°C for 30 min. Cells were filtered, centrifuged and plated on collagen-coated dishes and cultured in growth medium [F10 Ham's medium (Gibco) supplemented with 20% fetal bovine serum, 5 ng/ml bFGF and 1% penicillin-streptomycin].

To determine the cell proliferation rate, early passages of primary myoblasts were seeded (50,000 cells per well) on six-well plates coated with collagen and counted at different time points (day 0 to day 7). Experiments were performed in triplicate for each primary culture from each genotype and for each time point.

Muscle injury and regeneration assay

Muscle injury was induced by injecting 50 μl snake venom cardiotoxin I (Ctx, Latoxan) (12 μmol/l in PBS) with 26 G needles into the left tibialis muscle of 6-week-old anesthetized males as described previously (Yan et al., 2003; Castets et al., 2011). For multiple regeneration assays, four successive Ctx injections were performed with an interval of 4 weeks between injections. Muscles were collected 7 days after the fourth Ctx injury, to extract RNA or perform histological analysis. The multiple regeneration experiment was performed three times on 5-6 male mice for each experiment and for each genotype.

RNA isolation and quantitative PCR assay

Total RNA was extracted using the Qiagen miRNeasy mini kit (Qiagen) with DNase treatment to remove the genomic DNA. 500 ng of total RNA was reverse-transcribed using the PrimeScript RT reagent kit (Takara). Quantitative real-time PCR was performed on 10 ng cDNA using SYBR Premix Ex Taq (Takara) in a LightCycler 480 apparatus (Roche). Gene expression levels were normalized to the geometric mean of the expression level of *Mrpl32*, *Sdha* and *EiF4a2* housekeeping genes, as determined by Genorm analysis (Vandesompele et al., 2002). Primer sequences used for this study are listed in Table S1.

Statistical analysis

Statistical analysis was performed using Prism software. Student's *t*-test, two-way ANOVA with Bonferroni post test and Kruskal–Wallis test with Dunn's post test were used, as indicated in the figure legends.

Author contributions

C.M., P.M., Y.L. and A.G. performed experiments and analyzed data. M.B. helped with Ctx injection of the mice. L.D. directed the project, analyzed data and wrote the manuscript. All authors contributed to critical reading and editing of the manuscript.

Supplementary information

Supplementary information available online at
http://dev.biologists.org/lookup/suppl/doi:10.1242/dev.131771/-/DC1

References

Al Adhami, H., Evano, B., Le Digarcher, A., Gueydan, C., Dubois, E., Parrinello, H., Dantec, C., Bouschet, T., Varrault, A. and Journot, L. (2015). A systems-level approach to parental genomic imprinting: the imprinted gene network includes extracellular matrix genes and regulates cell cycle exit and differentiation. *Genome Res.* **25**, 353-367.

Andersen, D. C., Petersson, S. J., Jørgensen, L. H., Bollen, P., Jensen, P. B., Teisner, B., Schroeder, H. D. and Jensen, C. H. (2009). Characterization of DLK1+ cells emerging during skeletal muscle remodeling in response to myositis, myopathies, and acute injury. *Stem Cells* **27**, 898-908.

Andersen, D. C., Laborda, J., Baladron, V., Kassem, M., Sheikh, S. P. and Jensen, C. H. (2013). Dual role of delta-like 1 homolog (DLK1) in skeletal muscle development and adult muscle regeneration. *Development* **140**, 3743-3753.

Berg, J. S., Lin, K. K., Sonnet, C., Boles, N. C., Weksberg, D. C., Nguyen, H., Holt, L. J., Rickwood, D., Daly, R. J. and Goodell, M. A. (2011). Imprinted genes that regulate early mammalian growth are coexpressed in somatic stem cells. *PLoS ONE* **6**, e26410.

Borensztein, M., Monnier, P., Court, F., Louault, Y., Ripoche, M.-A., Tiret, L., Yao, Z., Tapscott, S. J., Forne, T., Montarras, D. et al. (2013). Myod and H19-Igf2 locus interactions are required for diaphragm formation in the mouse. *Development* **140**, 1231-1239.

Brannan, C. I., Dees, E. C., Ingram, R. S. and Tilghman, S. M. (1990). The product of the H19 gene may function as an RNA. *Mol. Cell. Biol.* **10**, 28-36.

Buckingham, M. (2007). Skeletal muscle progenitor cells and the role of Pax genes. *C. R. Biol.* **330**, 530-533.

Buckingham, M. and Relaix, F. (2007). The role of Pax genes in the development of tissues and organs: Pax3 and Pax7 regulate muscle progenitor cell functions. *Annu. Rev. Cell Dev. Biol.* **23**, 645-673.

Cao, Y., Yao, Z., Sarkar, D., Lawrence, M., Sanchez, G. J., Parker, M. H., MacQuarrie, K. L., Davison, J., Morgan, M. T., Ruzzo, W. L. et al. (2010). Genome-wide MyoD binding in skeletal muscle cells: a potential for broad cellular reprogramming. *Dev. Cell* **18**, 662-674.

Castets, P., Bertrand, A. T., Beuvin, M., Ferry, A., Le Grand, F., Castets, M., Chazot, G., Rederstorff, M., Krol, A., Lescure, A. et al. (2011). Satellite cell loss and impaired muscle regeneration in selenoprotein N deficiency. *Hum. Mol. Genet.* **20**, 694-704.

Charlier, C., Segers, K., Karim, L., Shay, T., Gyapay, G., Cockett, N. and Georges, M. (2001). The callipyge mutation enhances the expression of coregulated imprinted genes in cis without affecting their imprinting status. *Nat. Genet.* **27**, 367-369.

Clark, D. L., Clark, D. I., Hogan, E. K., Kroscher, K. A. and Dilger, A. C. (2015). Elevated insulin-like growth factor 2 expression may contribute to the hypermuscular phenotype of myostatin null mice. *Growth Horm. IGF Res.* **25**, 207-218.

Cooper, W. N., Luharia, A., Evans, G. A., Raza, H., Haire, A. C., Grundy, R., Bowdin, S. C., Riccio, A., Sebastio, G., Bliek, J. et al. (2005). Molecular subtypes and phenotypic expression of Beckwith-Wiedemann syndrome. *Eur. J. Hum. Genet.* **13**, 1025-1032.

Davis, R. L., Weintraub, H. and Lassar, A. B. (1987). Expression of a single transfected cDNA converts fibroblasts to myoblasts. *Cell* **51**, 987-1000.

Davis, E., Jensen, C. H., Schroder, H. D., Farnir, F., Shay-Hadfield, T., Kliem, A., Cockett, N., Georges, M. and Charlier, C. (2004). Ectopic expression of DLK1 protein in skeletal muscle of padumnal heterozygotes causes the callipyge phenotype. *Curr. Biol.* **14**, 1858-1862.

Dey, B. K., Pfeifer, K. and Dutta, A. (2014). The *H19* long noncoding RNA gives rise to microRNAs miR-675-3p and miR-675-5p to promote skeletal muscle differentiation and regeneration. *Genes Dev.* **28**, 491-501.

Gabory, A., Ripoche, M.-A., Le Digarcher, A., Watrin, F., Ziyyat, A., Forne, T., Jammes, H., Ainscough, J. F. X., Surani, M. A., Journot, L. et al. (2009). H19 acts as a trans regulator of the imprinted gene network controlling growth in mice. *Development* **136**, 3413-3421.

Gabory, A., Jammes, H. and Dandolo, L. (2010). The H19 locus: role of an imprinted non-coding RNA in growth and development. *Bioessays* **32**, 473-480.

Grobet, L., Royo Martin, L. J., Poncelet, D., Pirottin, D., Brouwers, B., Riquet, J., Schoeberlein, A., Dunner, S., Ménissier, F., Massabanda, J. et al. (1997). A deletion in the bovine myostatin gene causes the double-muscled phenotype in cattle. *Nat. Genet.* **17**, 71-74.

Haig, D. (2004). Genomic imprinting and kinship: how good is the evidence? *Annu. Rev. Genet.* **38**, 553-585.

Hao, Y., Crenshaw, T., Moulton, T., Newcomb, E. and Tycko, B. (1993). Tumour-suppressor activity of H19 RNA. *Nature* **365**, 764-767.

Jerkovic, R., Argentini, C., Serrano-Sanchez, A., Cordonnier, C. and Schiaffino, S. (1997). Early myosin switching induced by nerve activity in regenerating slow skeletal muscle. *Cell Struct. Funct.* **22**, 147-153.

Kalista, S., Schakman, O., Gilson, H., Lause, P., Demeulder, B., Bertrand, L., Pende, M. and Thissen, J. P. (2012). The type 1 insulin-like growth factor receptor (IGF-IR) pathway is mandatory for the follistatin-induced skeletal muscle hypertrophy. *Endocrinology* **153**, 241-253.

Kallen, A. N., Zhou, X.-B., Xu, J., Qiao, C., Ma, J., Yan, L., Lu, L., Liu, C., Yi, J.-S., Zhang, H. et al. (2013). The imprinted H19 lncRNA antagonizes let-7 microRNAs. *Mol. Cell* **52**, 101-112.

Keniry, A., Oxley, D., Monnier, P., Kyba, M., Dandolo, L., Smits, G. and Reik, W. (2012). The H19 lincRNA is a developmental reservoir of miR-675 that suppresses growth and Igf1r. *Nat. Cell Biol.* **14**, 659-665.

Kishioka, Y., Thomas, M., Wakamatsu, J.-I., Hattori, A., Sharma, M., Kambadur, R. and Nishimura, T. (2008). Decorin enhances the proliferation and

DEVELOPMENT

differentiation of myogenic cells through suppressing myostatin activity. *J. Cell Physiol.* **215**, 856-867.

Le Grand, F., Grifone, R., Mourikis, P., Houbron, C., Gigaud, C., Pujol, J., Maillet, M., Pages, G., Rudnicki, M., Tajbakhsh, S. et al. (2012). Six1 regulates stem cell repair potential and self-renewal during skeletal muscle regeneration. *J. Cell Biol.* **198**, 815-832.

Lee, S.-J. and McPherron, A. C. (2001). Regulation of myostatin activity and muscle growth. *Proc. Natl. Acad. Sci. USA* **98**, 9306-9311.

Legnini, I., Morlando, M., Mangiavacchi, A., Fatica, A. and Bozzoni, I. (2014). A feedforward regulatory loop between HuR and the long noncoding RNA linc-MD1 controls early phases of myogenesis. *Mol. Cell* **53**, 506-514.

Lui, J. C., Finkielstain, G. P., Barnes, K. M. and Baron, J. (2008). An imprinted gene network that controls mammalian somatic growth is down-regulated during postnatal growth deceleration in multiple organs. *Am. J. Physiol. Regul. Integr. Comp. Physiol. Rev.* **295**, R189-R196.

Monnier, P., Martinet, C., Pontis, J., Stancheva, I., Ait-Si-Ali, S. and Dandolo, L. (2013). H19 lncRNA controls gene expression of the imprinted gene network by recruiting MBD1. *Proc. Natl. Acad. Sci. USA* **110**, 20693-20698.

Musarò, A., McCullagh, K., Paul, A., Houghton, L., Dobrowolny, G., Molinaro, M., Barton, E. R., Sweeney, H. L. and Rosenthal, N. (2001). Localized Igf-1 transgene expression sustains hypertrophy and regeneration in senescent skeletal muscle. *Nat. Genet.* **27**, 195-200.

Pallafacchina, G., François, S., Regnault, B., Czarny, B., Dive, V., Cumano, A., Montarras, D. and Buckingham, M. (2010). An adult tissue-specific stem cell in its niche: a gene profiling analysis of in vivo quiescent and activated muscle satellite cells. *Stem Cell Res.* **4**, 77-91.

Pasut, A., Jones, A. E. and Rudnicki, M. A. (2013). Isolation and culture of individual myofibers and their satellite cells from adult skeletal muscle. *J. Vis. Exp.* **73**, e50074.

Pelosi, L., Giacinti, C., Nardis, C., Borsellino, G., Rizzuto, E., Nicoletti, C., Wannenes, F., Battistini, L., Rosenthal, N., Molinaro, M. et al. (2007). Local expression of IGF-1 accelerates muscle regeneration by rapidly modulating inflammatory cytokines and chemokines. *FASEB J.* **21**, 1393-1402.

Pfeifer, K. and Tilghman, S. M. (1994). Allele-specific gene expression in mammals: the curious case of the imprinted RNAs. *Genes Dev.* **8**, 1867-1874.

Poirier, F., Chan, C.-T. J., Timmons, P. M., Robertson, E. J., Evans, M. J. and Rigby, P. W. J. (1991). The murine H19 gene is activated during embryonic stem cell differentiation *in vitro* and at the time of implantation in the developing embryo. *Development* **113**, 1105-1114.

Ripoche, M. A., Kress, C., Poirier, F. and Dandolo, L. (1997). Deletion of the H19 transcription unit reveals the existence of a putative imprinting control element. *Genes Dev.* **11**, 1596-1604.

Sabourin, L. A. and Rudnicki, M. A. (2000). The molecular regulation of myogenesis. *Clin. Genet.* **57**, 16-25.

Sambasivan, R. and Tajbakhsh, S. (2007). Skeletal muscle stem cell birth and properties. *Semin. Cell Dev. Biol.* **18**, 870-882.

Schultz, E., Gibson, M. C. and Champion, T. (1978). Satellite cells are mitotically quiescent in mature mouse muscle: an EM and radioautographic study. *J. Exp. Zool.* **206**, 451-456.

Smits, G., Mungall, A. J., Griffiths-Jones, S., Smith, P., Beury, D., Matthews, L., Rogers, J., Pask, A. J., Shaw, G., VandeBerg, J. L. et al. (2008). Conservation of the H19 noncoding RNA and H19-IGF2 imprinting mechanism in therians. *Nat. Genet.* **40**, 971-976.

Vandesompele, J., De Preter, K., Pattyn, F., Poppe, B., Van Roy, N., De Paepe, A. and Speleman, F. (2002). Accurate normalization of real-time quantitative RT-PCR data by geometric averaging of multiple internal control genes. *Genome Biol.* **3**, RESEARCH0034.

Varrault, A., Gueydan, C., Delalbre, A., Bellmann, A., Houssami, S., Aknin, C., Severac, D., Chotard, L., Kahli, M., Le Digarcher, A. et al. (2006). Zac1 regulates an imprinted gene network critically involved in the control of embryonic growth. *Dev. Cell* **11**, 711-722.

Venkatraman, A., He, X. C., Thorvaldsen, J. L., Sugimura, R., Perry, J. M., Tao, F., Zhao, M., Christenson, M. K., Sanchez, R., Yu, J. Y. et al. (2013). Maternal imprinting at the H19-Igf2 locus maintains adult haematopoietic stem cell quiescence. *Nature* **500**, 345-349.

Waddell, J. N., Zhang, P., Wen, Y., Gupta, S. K., Yevtodiyenko, A., Schmidt, J. V., Bidwell, C. A., Kumar, A. and Kuang, S. (2010). Dlk1 is necessary for proper skeletal muscle development and regeneration. *PLoS ONE* **5**, e15055.

Whalen, R. G., Harris, J. B., Butler-Browne, G. S. and Sesodia, S. (1990). Expression of myosin isoforms during notexin-induced regeneration of rat soleus muscles. *Dev. Biol.* **141**, 24-40.

White, R. B., Biérinx, A.-S., Gnocchi, V. F. and Zammit, P. S. (2010). Dynamics of muscle fibre growth during postnatal mouse development. *BMC Dev. Biol.* **10**, 21.

Yan, Z., Choi, S., Liu, X., Zhang, M., Schageman, J. J., Lee, S. Y., Hart, R., Lin, L., Thurmond, F. A. and Williams, R. S. (2003). Highly coordinated gene regulation in mouse skeletal muscle regeneration. *J. Biol. Chem.* **278**, 8826-8836.

Yoshimizu, T., Miroglio, A., Ripoche, M.-A., Gabory, A., Vernucci, M., Riccio, A., Colnot, S., Godard, C., Terris, B., Jammes, H. et al. (2008). The H19 locus acts in vivo as a tumor suppressor. *Proc. Natl. Acad. Sci. USA* **105**, 12417-12422.
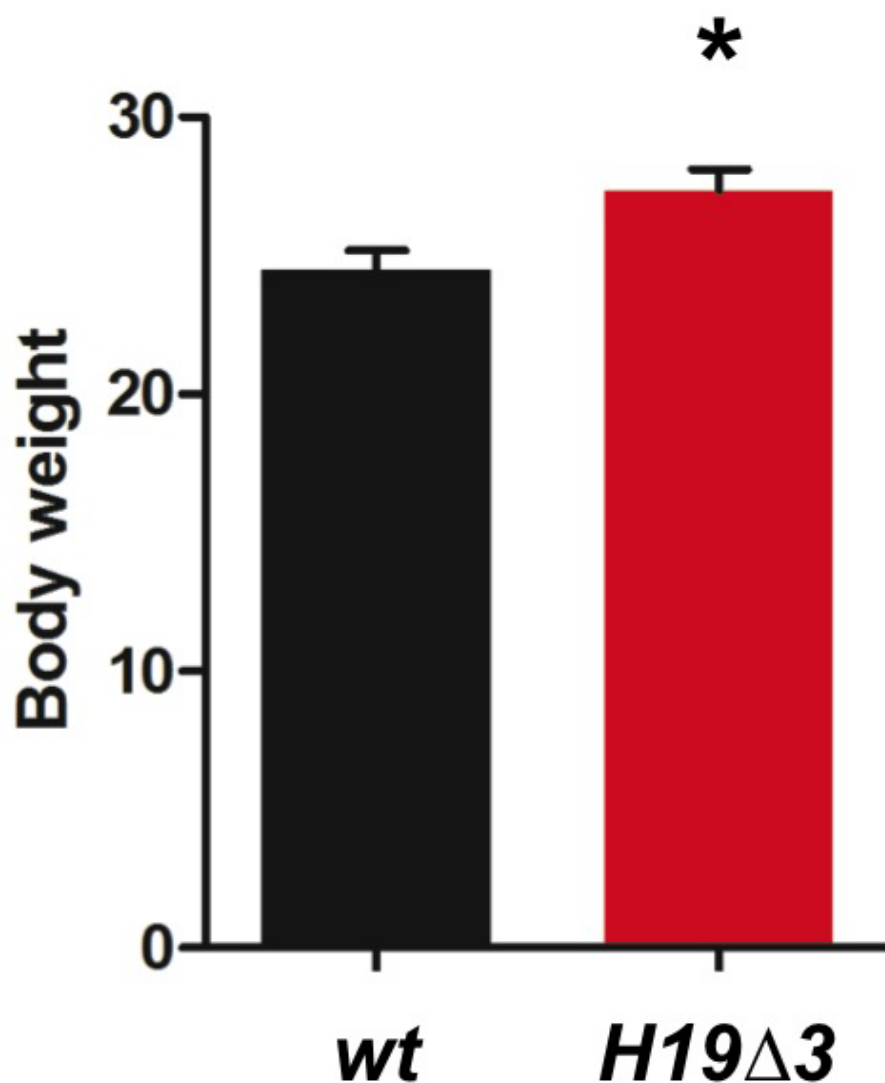
DEVELOPMENT

Figure S1. Adult *H19*^Δ3^ mice show an overgrowth phenotype.

Body weight of adult (4 months) *wt* and *H19*^Δ3^ mice (respectively n=16 mice and n=14 mice). Data are shown as mean ± SEM. Asterisk indicates statistically significant data (*, *p*<0.05 Student's *t*-test).
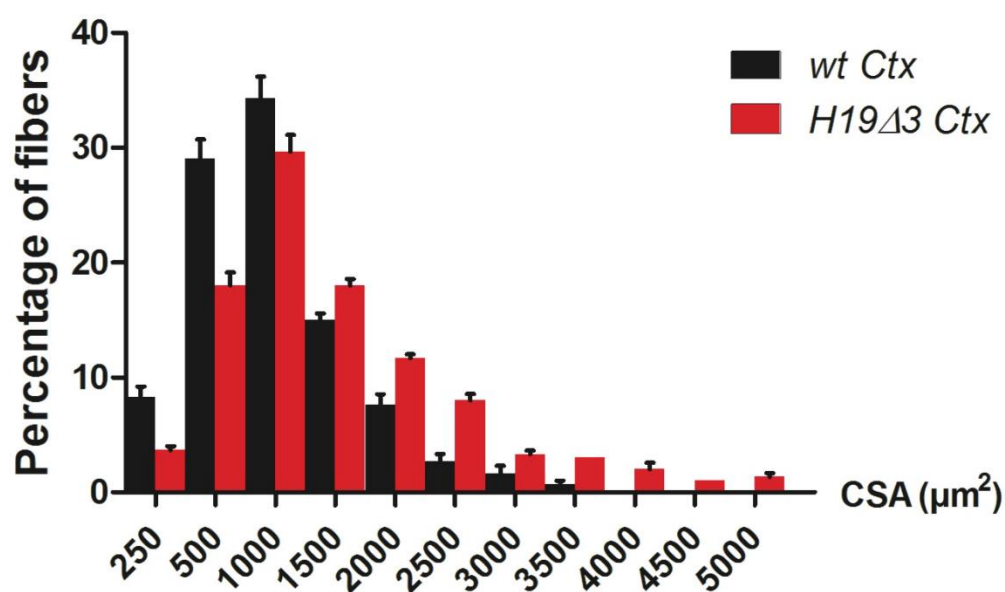
Figure S2. Regeneration assay after one Ctx injection.

Histogram of fiber CSA (μm^2) from injured adult *wt* and *H19$^{\Delta 3}$* *tibialis* muscles (n=3/genotype). Data are shown as mean ± SEM.
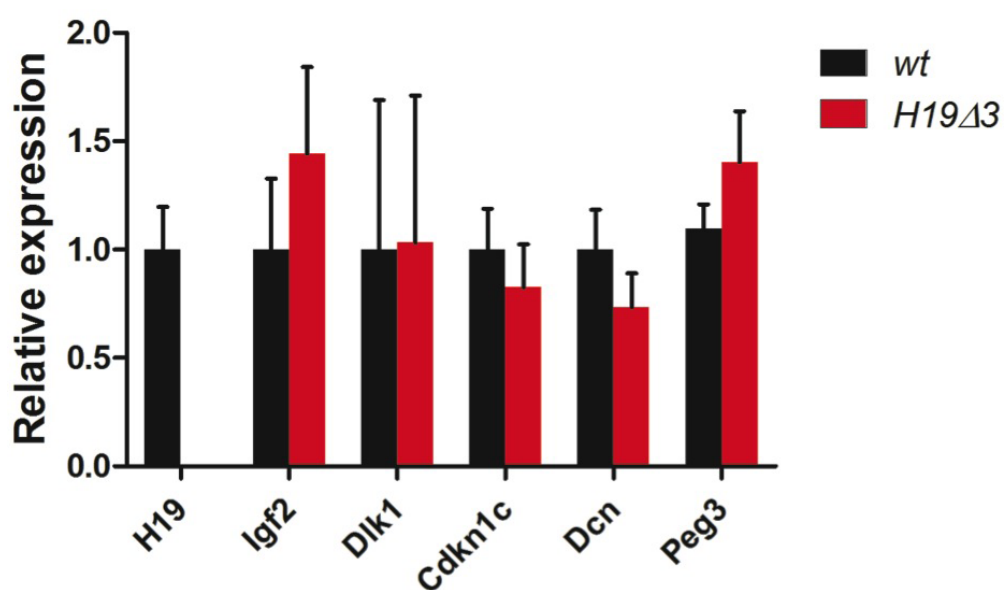
Figure S3. IGN expression in P21 myoblasts.

Transcript levels of the IGN genes in *wt* and *H19^{Δ3}* myoblasts (n=4 primary myoblast cultures/genotype). Data are shown as mean ± SEM.
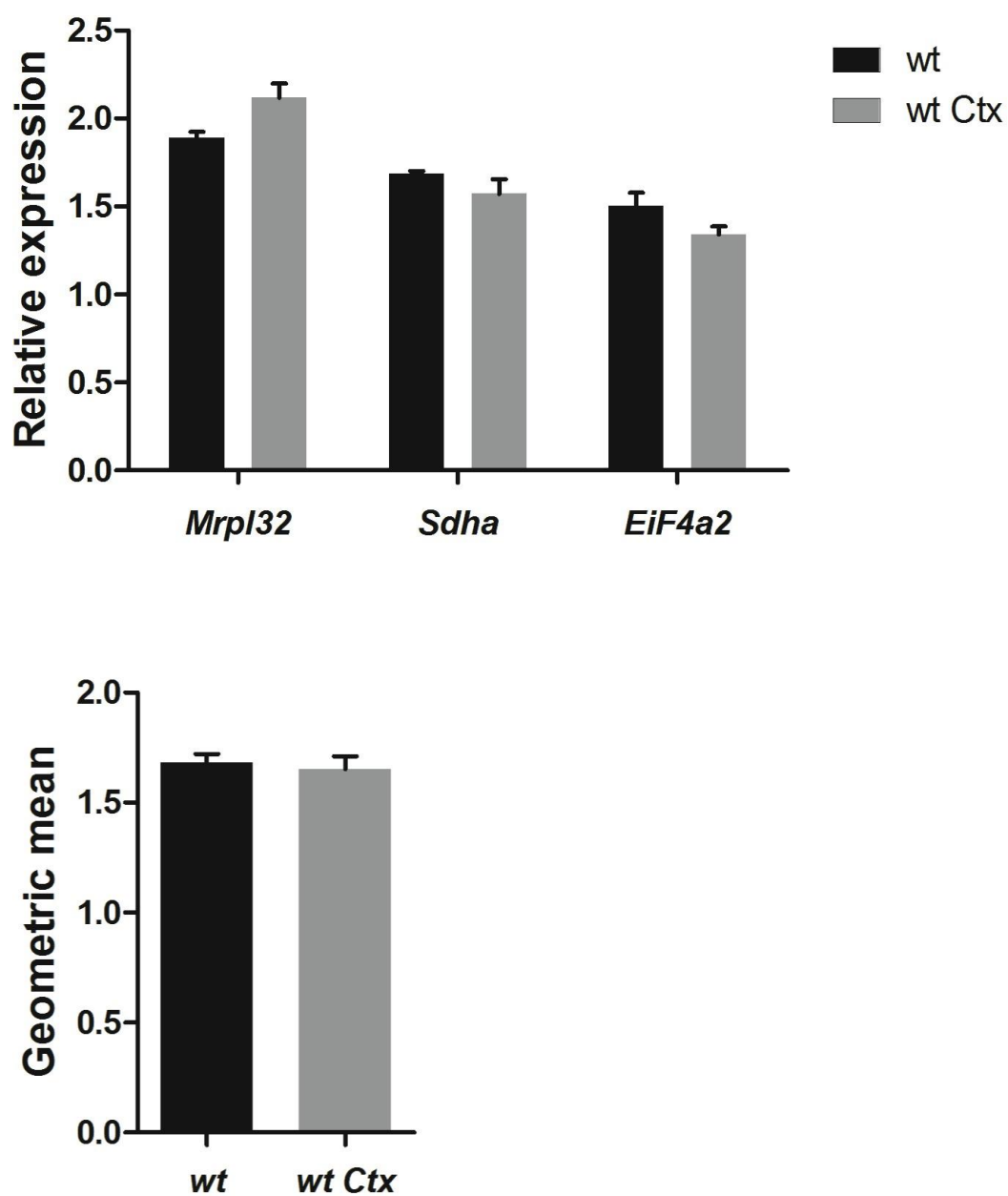
Figure S4. Transcript levels of reference genes.

RT-qPCR data for the three reference genes in control and Ctx-injected *tibialis* muscle samples. Data are shown as mean ± SEM.
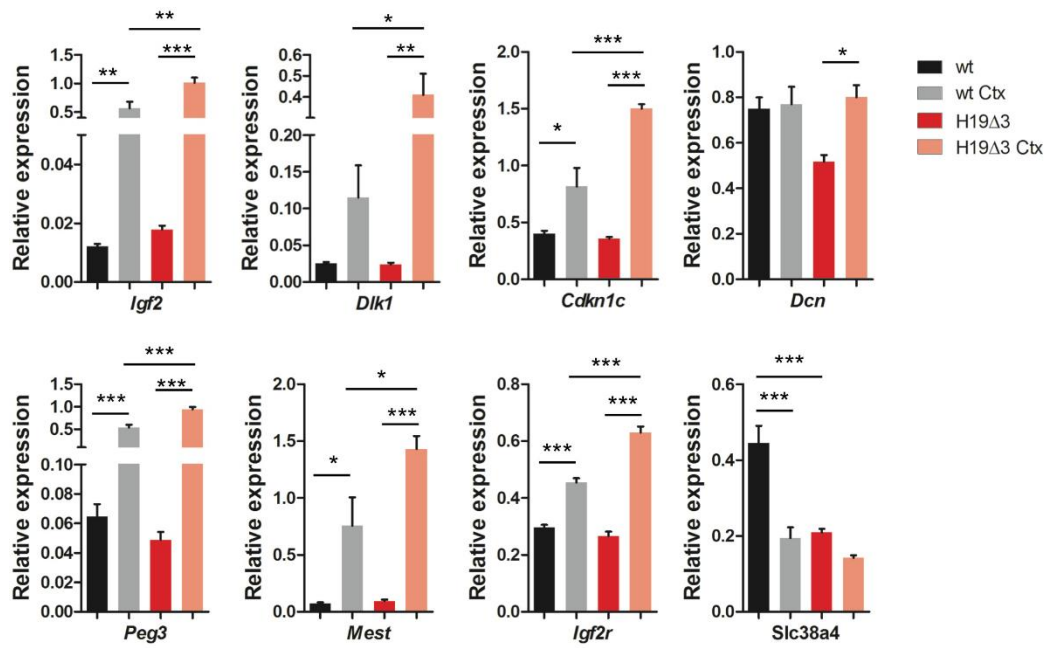
Figure S5. IGN expression in muscle regeneration.

Transcript levels of the IGN genes in *wt* and *H19^{Δ3}* adult *tibialis* muscles (n=4 mice/genotype). Data are shown as mean ± SEM. Asterisks indicate statistically significant data (*, $p<0.05$; **, $p<0.01$; ***, $p<0.001$ one-way Anova with Bonferroni post test).
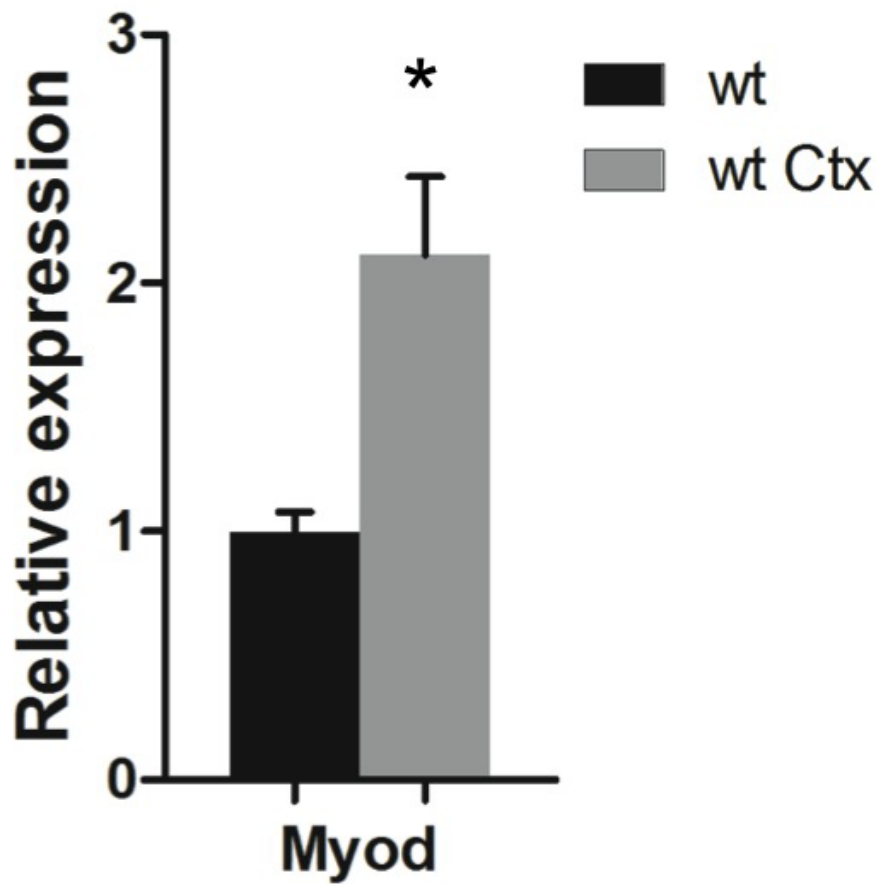
Figure S6. *Myod* gene is overexpressed after Ctx injury in *wt* mice.

Transcript levels of the *Myod* gene in *wt* and *H19^{Δ3}* adult *tibialis* muscles (n=4 mice/genotype). Data are shown as mean ± SEM. Asterisk indicates statistically significant data (*, $p<0.05$ Student's *t*-test).

Table S1: Primers used for Real Time RT-PCR

Gene	Forward Primer 5'-3'	Reverse Primer 5'-3'
H19	GGAGACTAGGCCAGGTCTC	GCCCATGGTGTTCAAGAAGGC
Igf2	GGTGCTTCTCATCTCTTTGG	CGACGGTTGGCACGGCTTGA
Igf2r	GCACAGAATCCAGACTAGCATTACA	CCTCCTTATCAGCTTTAAATATGTCTTTCTT
Igf1	CACTCATCCACAATGCCTGT	TGGATGCTCTTCAGTTCGTG
Igf1r	GTGGGGGCTCGTGTTTCTC	GATCACCGTGCAGTTTTCCA
Dlk1	ACTTGCGTGGACCTGGAGAA	CTGTTGGTTGCGGCTACGAT
Cdkn1c	AACTTCCAGCAGGATGTGCC	CATCCACTGCAGACGACCAG
Dcn	CATCTTCGAGTGGTGCAGTGTT	GCAGGTCTAGCAAGGTTGTGTC
Peg3	TTGGACTGGACAGAGATGATGACA	ATTCTGGTATGACTCGGCATCCT
Mest/Peg1	CAACAATGACGGCAACCTGGT	TCTGAATTTCTTCCTTTGATTAATGTACTGTA
Slc38a4	ACTGTGGCAATACTCTCGCTCTA	ATCCAAATGCTTTCTCGCCCAAT
MyoD	GATGGTGCCCCTGGTTCTT	AAAGGCTTCGAAAGGACAGTT
Ki67	CAGTTTGGCGACATTAGCAGA	GCAACTATCTTGGCAACATCCTC
Pax7	TGTCTCCAAGATTCTGTGCC	GGATTTCCCAGCTGAACATC